Chalcogenide Letters Vol. 12, No. 2, February 2015, p. 43 - 50

STRUCTURAL, OPTICAL AND ELECTRICAL PROPERTIES OF NANOCRYSTALLINE CdS THIN FILMS GROWN BY CHEMICAL BATH DEPOSITION METHOD

R. DEMIR[a*], F. GODE[b]
[a]*Vocational School of Technical Science, Çanakkale Onsekiz Mart University,17020 Çanakkale, Turkey*
[b]*Department of Physics, Mehmet Akif Ersoy University, 15030 Burdur, Turkey*

Cadmium sulfide thin films are prepared on glass substrates at 82 °C for 1 hour by chemical bath deposition. After deposition, the films are annealed at 480 °C for 1 hour in air atmosphere. Both as-grown and annealed films are characterized by X-ray diffraction, scanning electron microscopy, energy dispersive spectroscopy, optical absorption spectroscopy and current voltage characteristics and their structural, morphological, compositional, optical and electrical properties are investigated. The X-ray diffraction patterns of deposited films show the formation of polycrystalline of CdS with both cubic and hexagonal structure. Moreover, after the thermal treatment of 480 °C, they mostly turn into polycrystalline CdO with cubic structure. The grain size of the deposited film decreases approximately from 10−20 nm to 2-3.5−5.5 nm by annealing. The band gap energy of the films is determined for the direct transitions of 2.15 eV and increased to 2.25 eV by the thermal treatment. After thermal process, the electrical conductivity of the films calculated from the current–voltage characteristic in the dark increases from 5.482×10^{-10} $(\Omega\ cm)^{-1}$ to 5.304×10^{-8} $(\Omega\ cm)^{-1}$. The observed conduction mechanism in both as-grown and annealed films is ohmic.

(Received December 27, 2015; Accepted February 2, 2015)

Keywords: CdS; Chemical Bath Deposition; Optical properties; Electrical properties

1. Introduction

In recent years, there has been growing interest in II–VI semiconductor materials for their potential applications in optoelectronic and photovoltaic industries. One of the most promising alternative materials is a cadmium sulfide (CdS) thin film, which is a chalcogenide n-type semiconductor having a direct energy band gap between 2.28 eV and 2.45 eV [1]. Owing to its interesting structural, optical and electrical properties that are much different compared to bulk materials, these films can be applied to many technologies such as window layer in solar cells [2], optical sensors [3], transistors [4], diodes [5], etc.

Various methods such as electro-deposition [6], spray pyrolysis [7], successive ionic layer adsorption and reaction (SILAR) [8], pulsed-laser deposition [9], vacuum evaporation [10] and chemical bath deposition (CBD) [11], etc. are used to obtain CdS thin films. Among these fabrication methods, CBD is known as the simplest and most economical method for the large-area productions in obtaining semiconductor thin films.

It is well known that CdS thin films may be exist in either cubic or hexagonal phase or as a mixture of both phases depending on many factors including deposition technique. The difficulty in the formation of nanocrystalline CdS thin films stems from a strong self-compensation effect due to sulfur vacancies and the depth of the acceptor level in CdS. Therefore, it is very important to vary morphological, optical and electrical properties of CdS thin films by adjusting the grain size for technological applications using low cost and an easy method. Hence, nanocrystalline CdS

*Corresponding author: rdemir@comu.edu.tr

thin films are deposited on glass substrates using CBD method. The films are annealed at 480 °C for 1 hour in air in order to get one single phase in the deposited films. The structural, morphological, compositional, optical and electrical properties of the as-grown and annealed CdS films are investigated.

2. Experimental details

The CdS thin films are deposited on glass substrates with the size of 76×26×1 mm^3. The substrates are previously washed out with a soapy solution, rinsed with de-ionized water, etched with diluted hydrochloric acid (5%), cleaned in de-ionized water and then cleaned with propanol, methanol and again washed with deionized water and finally dried in flowing air. For depositing the CdS thin films, a basic chemical bath solution consists of 10 ml of 0.2 M cadmium chloride ($CdCl_2.H_2O$), 10 ml of 0.48 M thiourea [$CS(NH_2)_2$], 8 ml buffer solution ammonia/ammonium chloride (NH3/NH4Cl; pH = 11.50).The total volume of the solution is completed to 50 ml by addition of de-ionized water. The films are obtained at 82 °C for 1 hour. Deposited films are air annealed at 480 °C for 1 hour in air atmosphere.

The chemical reaction to deposit CdS films may be written as follows:

$$Cd(NH_3)_4^{2+} \leftrightarrow 4NH_3 + Cd^{2+} \quad (1)$$

$$NH_3 + H_2O \leftrightarrow NH_4 + OH^- \quad (2)$$

$$CS(NH_2)_2 + OH^- \leftrightarrow SH^- + CH_2N_2 + H_2O \quad (3)$$

$$SH^- + OH^- \leftrightarrow S^{2-} + H_2O \quad (4)$$

$$Cd^{2+} + S^{2-} \leftrightarrow CdS \quad (5)$$

From the above reaction, the main role of NH_3 concentration in the bath is as complexing agent for the Cd^{2+} ions. The NH_3 concentration in the reaction solution is one of the control parameters in the growth rate of CdS films.

In the present study, the thickness of the deposited film is determined as 1233 nm by a weight gravimetric method using a density value of 4.82 g/cm^3 for the bulk CdS. The X-ray diffraction study is carried out using Rigaku Rint 2000 with Cu-K_α radiation (λ = 1.5418 Å) in the 2θ range from 20° to 70°. The surface morphology is performed by means of a ZEISS scanning electron microscope (SEM). Film composition is analyzed using an energy dispersive X-ray (EDX) analysis set up attached to SEM. The optical measurements of the films are recorded using UV–Visible Shimadzu Solid Spec-3700 DUV, UV-VIS-NIR spectrophotometer in the wavelength range of 300–2500 nm at room temperature. The current-voltage (I-V) characteristics of the films are studied in the dark using Hewlett-Packard 4140B Model pA Meter/DC voltage source.

3. Results and discussion

3.1. Structural properties

The XRD pattern of as-grown and annealed CdS thin films is presented in Fig. 1. It is clearly seen that both deposited and annealed films are polycrystalline in nature. Comparing XRD results with reference data for cubic and hexagonal CdS crystalline phases, it can be observed that as-grown film has diffraction peaks at 25.03°, 26.62° and 28.36°, corresponding to the (100), (002) and (101) planes, respectively for the CdS phase with hexagonal structure (PDF No. 41-1049), and the other peaks located at 44.05° and 52.33°, corresponding to the (220) and (311) planes, respectively for the CdS phase with cubic one (PDF No. 10-0454) in Fig. 1. The structural data for

as-grown films are in good agreement with the earlier report presented by Hernández-Borja et al [12], in which CdS thin films are produced on conducting glass/ITO substrates by the CBD method. Moreover, Nazir et al [13] observed both cubic and hexagonal phase in CdS thin films using Close Spaced Sublimation (CSS) technique. Ziabari et al [14] obtained a mixed (cubic/hexagonal) crystal structure of CdS thin films deposited by sol-gel method. Ghosh et al [15] found a mixed phase of both cubic and hexagonal structure in CdS films produced by CBD.

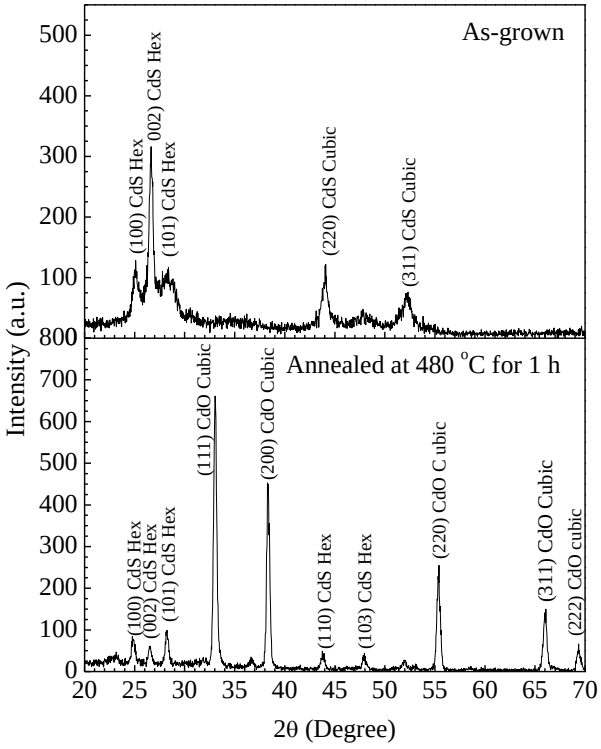

Fig. 1: XRD patterns of the as-grown and annealed CdS thin films.

Annealed film indicates five strong reflections around 33.04°, 38.32°, 55.36°, 66.01° and 69.34° corresponding to the (111), (200), (220), (311) and (222) planes, respectively for the CdO phase with cubic structure (PDF No. 05-0640). Moreover, it shows five less intensity diffraction peaks at 24.85°, 26.50°, 28.21°, 43.81° and 47.92°, which are related to (100), (002), (101), (110) and (103) crystalline planes of hexagonal CdS, respectively in Fig 1. It is seen that majority of crystallite belongs to the cubic phase of CdO. Therefore, we conclude that the annealed films mostly turn into a cubic crystal structure of CdO as well as the stable hexagonal crystal structures of CdS. Chun et al [16] found the hexagonal of CdS thin films varied into cubic CdO after $CdCl_2$ heat treatment.

Scanning electron micrographs of as-deposited and annealed CdS thin films with different magnitudes are shown in Fig. 2. As can be seen from Fig. 2(a) and (b), the obtained film is dense and shows a strong adherence to the surface. It can also be seen from these figures that the deposited film surface is smooth, homogeneous, continuous and the substrate is well covered by CdS nanoparticles in the range about 10–20 nm. Thermal process reveals the presence of agglomerated spherical shaped with voids, distinct nanoparticles approximately between 3.5–5.5 nm in Fig. 2(c) and (d). The SEM image of as-deposited film is similar to the earlier data [17]. It is clearly seen from the XRD and SEM results that the annealing process modifies the crystallite structure and leads to a reduction in size of the nanoparticles.

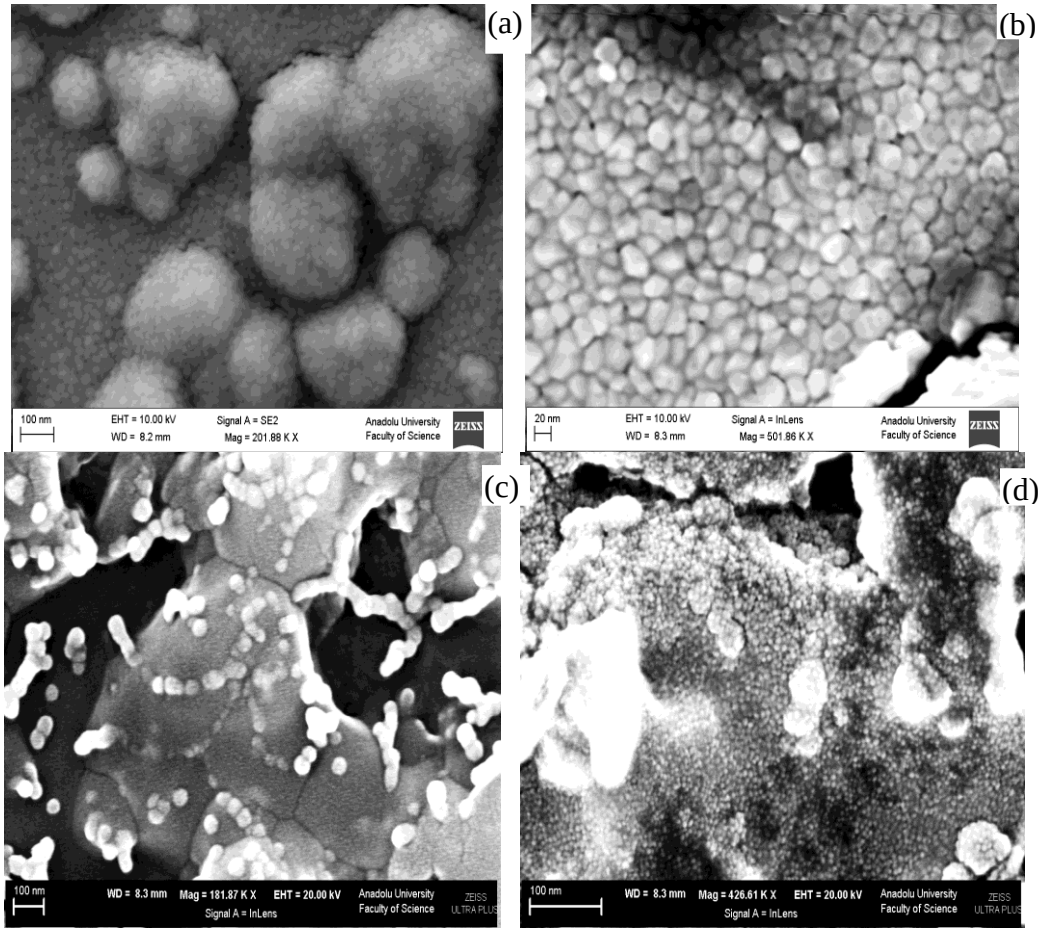

Fig. 2: SEM images of nanocrstalline CdS thin films with different magnifications: (a, b) as-grown and (c, d) annealed.

The compositional study was carried to obtain the elemental composition in as-deposited and annealed CdS films using energy dispersive X-ray spectrum (EDX) as shown in Fig. 3. The elemental analysis is carried out only for Cd, S and O elements. After thermal process at 480 °C for 1 hour, the average atomic ratio of S/Cd in the film decreases from 0.88 to 0.85 and the surface of the films is cadmium rich. Also, the atomic percentage (%) of oxygen decreases from 36.63 to 36.14.

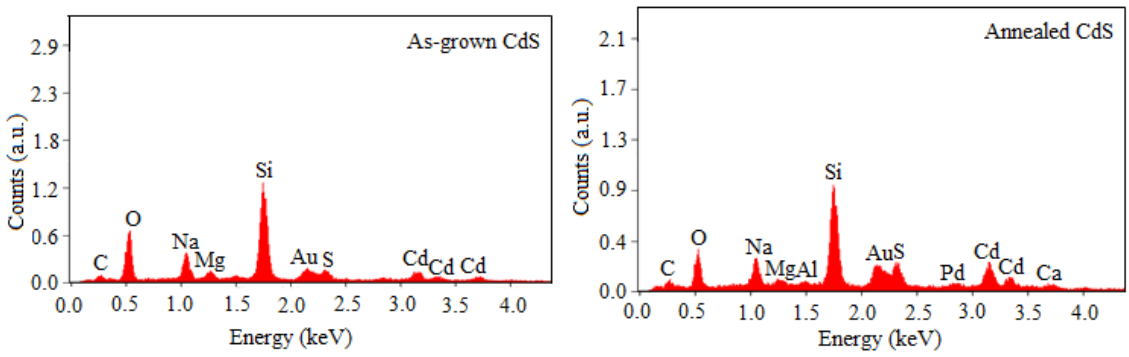

Fig. 3: EDX analysis on the surface of as-deposited and annealed CdS thin films.

3.2. Optical properties

Optical absorbance and transmittance spectra in the UV–visible regions of the as-grown and annealed CdS thin films are shown in Fig. 4(a) and (b), respectively. After thermal process, transparency decreases in the visible region.

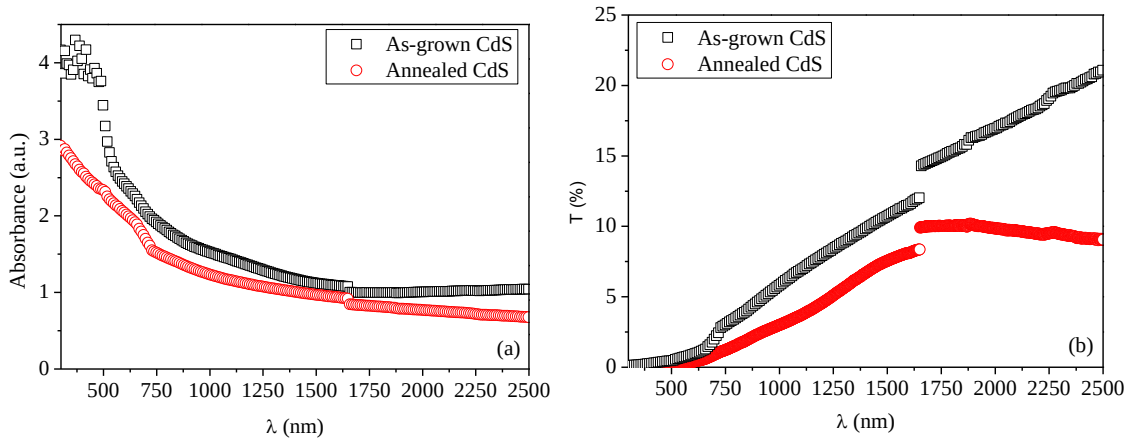

Fig. 4: The dependence of (a) absorption and (b) transmission spectra of as-grown and annealed films on the wavelength.

The band gap energy (E_g) of the films is derived by using the Tauc relation [18]:

$$(\alpha h\nu)^2 = K\left(h\nu - E_g\right) \tag{6}$$

where K is a constant and E_g is the band gap energy. The absorption coefficient (α) which is a function of the photon energy ($h\nu$) is calculated from the optical transmittance spectra results using the following equation [19]:

$$\alpha = -lnT/d \tag{7}$$

where d is the thickness of the film and T is the optical transmittance. The E_g value is determined by extrapolating the linear part of the plot $(\alpha h\nu)^2$ versus $(h\nu)$ in the abscissa (x axis), which indicates a direct optical transition. The $(\alpha h\nu)^2$ versus $(h\nu)$ plots for both as-prepared and annealed CdS films are shown in Fig. 5. As can be seen from this figure, band gap energy of the film increases from 2.15 eV to 2.25 eV with annealing due to the variation of film stoichiometry associated with the affinity of Cd towards oxygen, shrinkage of strain, reduction in grain size, enhancement the width of grain boundaries, the oxidized compounds at the surface of films, whereas Maticiuc et al [20] reported that the band gap energy of air-annealed CdS thin film decreases from 2.4 eV to 2.34 eV. They also heated the CdS films in H_2 medium at 400 °C for 1 hour and observed a reduction in the band gap value from 2.33 eV to 2.30 eV in [21]. The optical band gap values of 2.15 eV and 2.25 eV are estimated for both as-deposited and annealed CdS films, which varies between E_g = 1.70 eV [22] and 2.72 eV [23] as reported earlier.

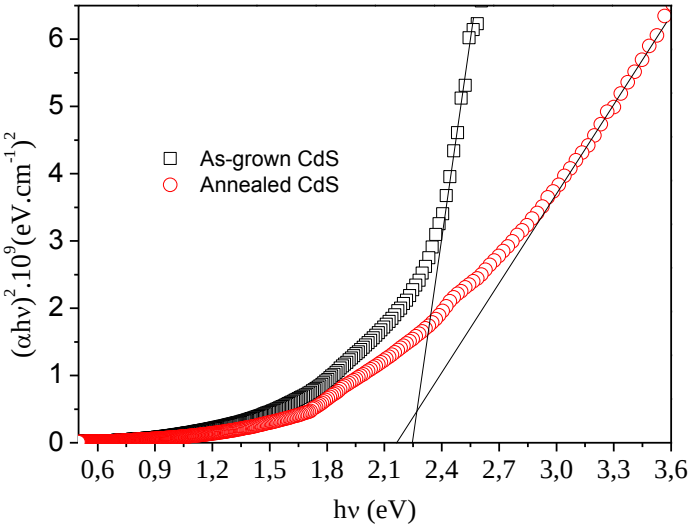

Fig. 5: The dependence of $(\alpha h\nu)^2$ on the photon energy (hν).

3.3. Electrical properties

Fig. 6 shows the schematic drawing of planar metal–semiconductor–metal (Au/CdS/Au) contacts which are made for studying current voltage characteristic of CdS films. Metal contacts are obtained by a vacuum evaporation method. The I-V measurements in dark are performed to investigate the conduction mechanisms and calculate the electrical conductivity in the voltage range of 0.1–100 V. Fig. 7 shows the I-V characteristic of as-grown and annealed CdS thin film. It is clearly seen from this figure that there is only one region with the same slope. The ohmic conduction is dominant in the whole voltage range where the slope is 1.0. The number of free carrier is more than that of the injected ones in this region.

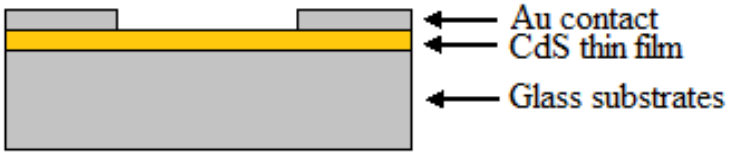

Fig. 6: Schematic drawing of planar Au/CdS/Au contacts.

As can be seen from this figure, electrical conductivity of as-grown film increases from 5.482×10^{-10} $(\Omega\ cm)^{-1}$ to 5.304×10^{-8} $(\Omega\ cm)^{-1}$ with annealing. This increase in electrical conductivity is due to incorporated oxygen on sulfur site and its reaction with Cd forms CdO phase in the film [21]. Atay et al [24] obtained a higher electrical conductivity [10^{-8} $(\Omega\ cm)^{-1}$] of CdS thin films in their work. In comparison with their data, the electrical conductivity of as-deposited CdS thin films is lower by about two orders of magnitude.

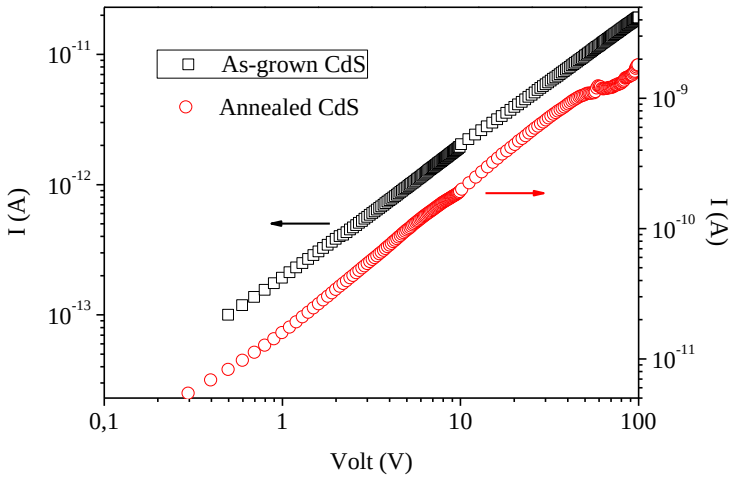

Fig. 7: The I-V characteristics of both as-deposited and annealed CdS thin films in the log-log scale.

4. Conclusion

Nanocrystalline CdS thin films are deposited on glass substrate by CBD technique. The films are annealed in air to improve its crystallinity. The XRD spectrum of as-deposited CdS films shows a polycrystalline and a mixed phase of both cubic and hexagonal structure with the size about 10–20 nm. However, annealing at 480 °C in air preserves the same structural hexagonal phase and results in transformation of CdS phase to CdO. SEM images illustrated that CdS nanoparticles decrease to approximately 3.5−5.5 nm after the heating treatment. Annealing process leads to a slow decrease in the S/Cd molar concentration of the film. Optical band gap energy of CdS films increases from 2.15 eV to 2.25 eV with annealing. The annealed films show a sharp increase in the electrical conductivity of two orders of magnitude because of the phase transformation (CdS→CdO). It can be concluded that annealing process changes the structural, optical and electrical properties of the CdS films.

References

[1] A. Kariper, E. Guneri, F. Gode, C. Gumus, T. Ozpozan, Mater. Chem. Phys. **129**, 183 (2011).
[2] H.A. Mohamed, Solar Energy **108**, 360 (2014).
[3] M. Husham, Z. Hassan, M.A. Mahdi, A.M. Selman, N.M. Ahmed, Superlattices Microstruct. **67**, 8 (2014).
[4] J.H Kwon, J.S. Ahn, H. Yang, Curr. Appl. Phys. **13**, 84 (2013).
[5] M. Tomakin, M. Altunbas, E. Bacaksız, Physica B **406**, 4355 (2011).
[6] C. Lu, L. Zhang, Y. Zhang, S. Liu, G. Liu, Appl. Surf. Sci. **319**, 278 (2014).
[7] S.J. Ikhmayies, R.N.A. Bitar, Appl. Surf. Sci. **256**, 3541 (2010).
[8] K. Gowrish Rao, V.K. Ashith, J. Phys. Chem. **Solids77**, 14 (2015).
[9] J.C. Orlianges, C. Champeaux, P. Dutheil, A. Catherinot, T.M. Mejean, Thin Solid Films **519**, 7611 (2011).
[10] M. Tomakin, M. Altunbaş, E. Bacaksiz, Ş. Çelik, Thin Solid Films **520**, 2532 (2012).
[11] S.U. Shaikh, F.Y. Siddiqui, D.J. Desale, A.V. Ghule, F. Singh, P.K. Kulriya, R. Sharma, Radiation Phys. Chem. **106**, 193 (2015).
[12] J. Hernández-Borja, Y.V. Vorobiev, R. Ramírez-Bon, Sol. Energy Mater. Sol. Cells **95**, 1882 (2011).
[13] A. Nazir, A. Toma, N. Abbas Shah, S. Panaro, S. Butt, R. ur Rehman Sagar, W. Raja, K. Rasool, A. Maqsood, J. Alloys Compd. **609**, 40 (2014).
[14] A.A. Ziabari, F.E. Ghodsi, Sol. Energy Mater. Sol. Cells **105**, 249 (2012).

[15] B. Ghosh, K. Kumar, B.K Singh, P. Banerjee, S. Das, Appl. Surf. Sci. **320**, 309 (2014).
[16] S. Chun, Y. Jung, J. Kim, D. Kim, J. Cryst. Growth **326**, 152 (2011).
[17] S. Butt, N.A. Shah, A. Nazir, Z. Ali, A. Maqsood, J. Alloys Compd. **587**, 582 (2014).
[18] T. Tauc, Amorphous and Liquid Semiconductor, Plenum Press, New York, 1974, 159.
[19] Y.P. Venkata Subbaiah, P. Prathap, K.T. Ramakrishna Reddy, Appl. Surf. Sci. **253,** 2409 (2006).
[20] N. Maticiuc, M. Kukk, N. Spalatu, T. Potlog, M. Krunks, V. Valdna, J. Hiie, Energy Procedia **44**, 77 (2014).
[21] N. Maticiuc, J. Hiie, T. Raadik, A. Graf, A. Gavrilov, Thin Solid Films **535**, 184 (2013).
[22] A. Izgorodin, O. Winther-Jensen, B. Winther-Jensen, D.R. MacFarlane, Phys. Chem. Chem. Phys. **11**, 8532 (2009).
[23] Ersin Yucel, Nuray Guler, Yasin Yucel, J. Alloys Comp. **589**, 207 (2014).
[24**]** F. Atay, S. Kose, V. Bilgin, I. Akyuz, Mater. Lett. **57**, 3461 (2003).